

CHAPTER 13

SHELLFISH HARVESTING STRATEGIES AT EL VARAL

DOUGLAS J. KENNETT AND BRENDAN J. CULLETON

EARLY FORMATIVE-PERIOD SITES ARE commonly found in peri-coastal and seasonally flooded wetland habitats in the Mazatán region (Lowe 1975; Blake 1991; Clark 1991, 1994). A similar distribution is evident in the Acapetahua and Pijijiapan regions to the northwest (Paillés 1980; Kennett et al. 2006), along the coast of Guatemala (Coe 1961; Coe and Flannery 1967; Love 1989, 1993; Arroyo 1994, 1995; Estrada Belli 1998), and into El Salvador (Arroyo 1995). Some of these sites were relatively sedentary fishing-farming communities (Kennett et al. 2002, 2006), whereas others (such as El Varal) appear to be more specialized locations for extracting resources from estuarine habitats.

Major economic and societal transformations occurred during the Early Formative period as people became more committed to maize-based food production (Kennett et al. 2006) and as institutionalized social hierarchies emerged (Clark and Blake 1994). Therefore, it is likely that the importance of estuarine resources varied regionally and temporally during this interval. This chapter assesses the seasonal periodicity of shellfish harvesting practices at El Varal using oxygen-isotope analysis of one mollusk species (*Polymesoda radiata*) collected at this location during the Early Formative period. The ultimate goal of this study was to assess the seasonality of occupation at the site.

BACKGROUND

Oxygen-isotope analysis of *P. radiata* shell carbonate is a well-established method for reconstructing pre-historic seasonal shellfish harvesting strategies along the Pacific Coast of southern Mexico (Kennett and Voorhies 1996). Previous work has focused in on Late Archaic-period (5500 to 4000 cal B.P.) subsistence and settlement strategies in the Acapetahua region 80 km northwest of El Varal (Figure 13.1), where a series of five large shell mounds are composed almost entirely of this marsh clam species (Voorhies 2004; Kennett et al. 2006).

The distribution and extent of these shell mounds suggests that the favored habitat of this species was more extensive between 5500 and 4000 cal B.P. Limited populations of *P. radiata* are still found today in Los Cerritos, the most landward lagoon in the Acapetahua Estuary and the most influenced by seasonal pulses of freshwater associated with wet-season rains between July and January.

Our work with *P. radiata* was originally founded upon the empirical observation that the stable oxygen-isotope composition of mollusk shells records aspects of their aquatic environment during growth (Wefer and Berger 1991). Changes in water temperature and salinity contribute to the isotopic composition of shell carbonate, with warmer water or inputs of low-salinity

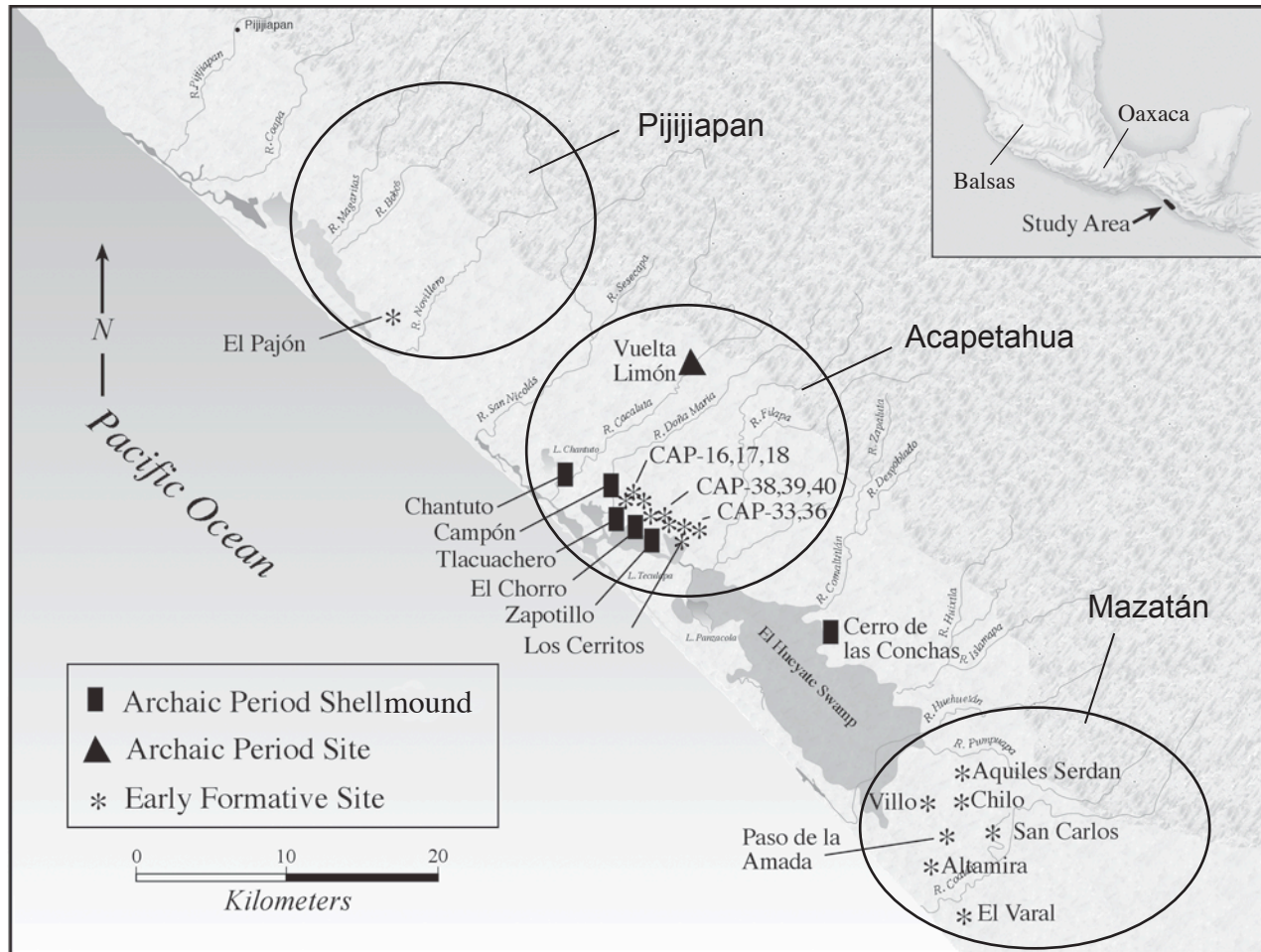


Figure 13.1. Map of the Pacific Coast of southern Mexico.

terrestrial runoff producing more-negative oxygen-isotope ($\delta^{18}\text{O}$) values (Epstein 1951, 1953; Shackleton 1973; Voorhies and Kennett 1995).

Kennett and Voorhies (1996) collected modern *P. radiata* specimens and water samples from the Los Cerritos Lagoon in the Acapetahua Estuary throughout one annual cycle to explore the environmental parameters influencing the stable oxygen and carbon isotopic records in their shells. They demonstrated that the final growth margin of these shells corresponded with the stable isotopic composition of the associated water sample (Figure 13.2), which in turn was linked to changes in water salinity and seasonal patterns of rainfall. More-negative oxygen-isotope values occurred during wet-season months, and more-positive values correlated with the dry season.

Water temperatures vary seasonally between 29.5 and 32.1° C (Voorhies 2004:13), but these contribute little to the overall oxygen-isotope composition of shell carbonate (Figure 13.2). Kennett and Voorhies

(1996:697–698) also determined that seasonal fluctuations in water salinity were also recorded through the incremental growth of individual *P. radiata* shells. The interpretation of carbon isotopes ($\delta^{13}\text{C}$) was more complex—reflecting the composition of available dissolved inorganic carbon (DIC) in the habitat, salinity, and “vital effects” related to growth, reproduction, and other confounding factors (Keith et al. 1964; Killingley and Berger 1979; Krantz et al. 1987; Kennett and Voorhies 1995, 1996). Carbon-isotope data are presented in Table 13.1, but these data are not interpreted or discussed in this chapter due to this complexity.

Prehistoric seasonal shellfish harvesting strategies are based on the observation that *P. radiata* shells faithfully record the summer monsoon. In the Acapetahua region, we have documented significant changes in shellfish harvesting practices during the Middle and Late Archaic periods (Kennett and Voorhies 1996; Voorhies et al. 2000). Marsh clams are available throughout the

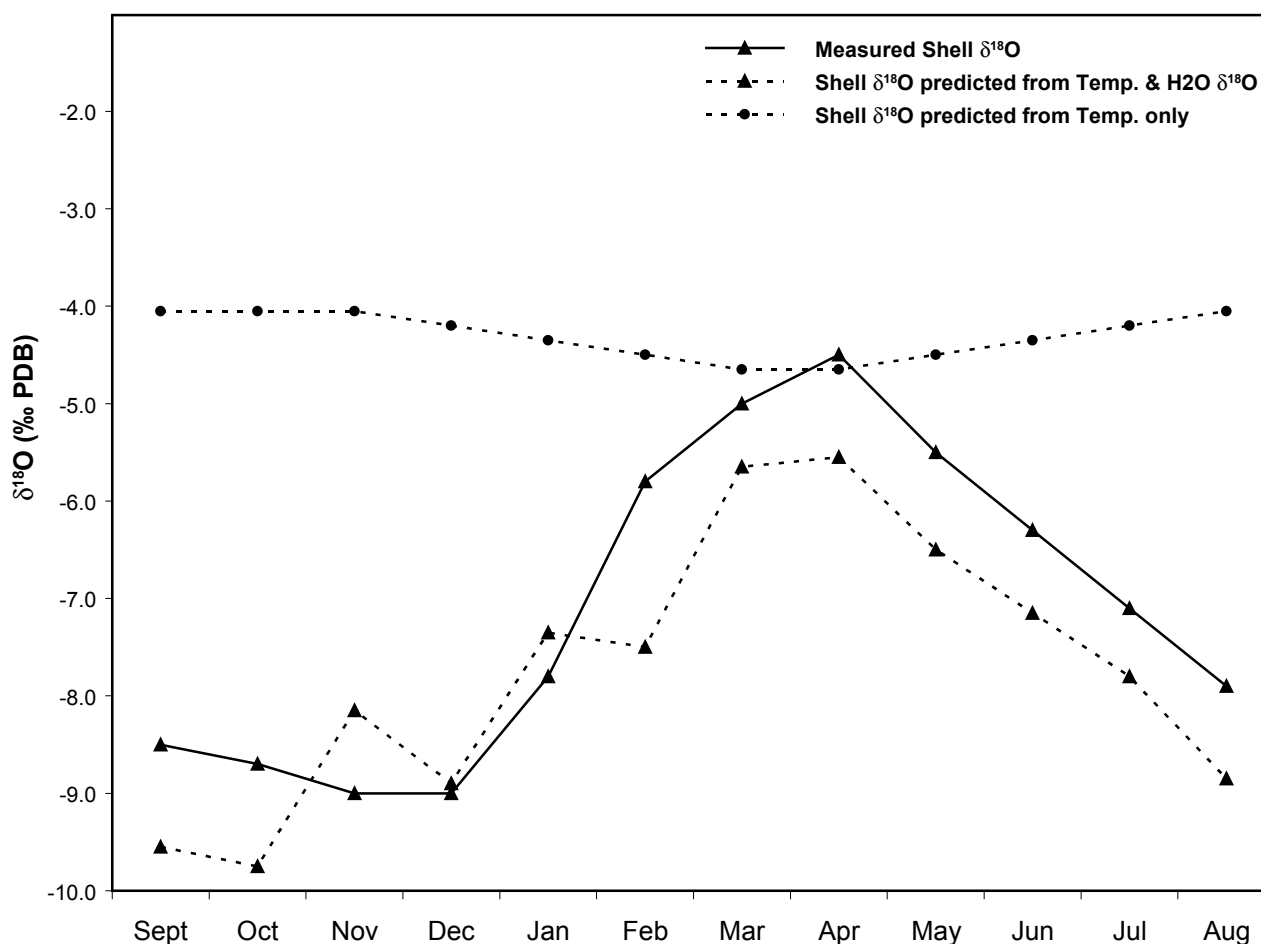


Figure 13.2. Measured and predicted shell $\delta^{18}\text{O}$ for Los Cerritos Lagoon (data from Kennett and Voorhies 1996; Voorhies 2004:13). Water temperature and water $\delta^{18}\text{O}$ values were used to model shell $\delta^{18}\text{O}$ according to the equation of Epstein et al. (1953), which agrees well with measured shell profile. Holding water $\delta^{18}\text{O}$ constant at -2‰ demonstrates the minor seasonal temperature effect, which makes most marine mollusks unsuitable for seasonality determination in the tropics.

year, but their collection may be sensitive to the use of estuarine settlements for other purposes. The overall abundance of resources increases in the Acapetahua Estuary during the dry season. Juvenile shrimp enter the estuary at this time, and a wider range of marine fishes preying upon them follows.

Marsh clams were collected throughout the year during the Middle and Late Archaic periods (7500 to 4500 cal B.P.), with a focus during the dry-season months. This is consistent with the idea that people were attracted to the fringe of this estuary primarily during the most productive time of the year. However, a major shift toward wet-season shellfish exploitation occurs at the end of the Late Archaic period that is synchronous with the first appearance of maize in these sequences (Kennett and Voorhies 1996; Kennett et al. 2006). This study provides a point of departure for interpreting the oxygen-isotope results from El Varal.

Table 13.1. Stable-isotope profile of *Polymesoda radiata*, N65W0/4, S29

Sample No.	Distance from Edge (mm)	$\delta^{13}\text{C}$ (PDB)	$\delta^{18}\text{O}$ (PDB)
EV2A	0	-7.20	-5.42
EV2B	2	-7.64	-7.50
EV2C	4	-6.85	-9.06
EV2D	6	-6.84	-9.32
EV2E	8	-7.64	-8.52
EV2F	10	-6.69	-8.68
EV2G	12	-6.42	-8.95
EV2H	14	-6.49	-10.50
EV2I	16	-6.78	-7.13
EV2J	18	-5.83	-3.52
EV2K	20	-5.43	-3.11

METHODS

In this study, intact valves of *P. radiata* shells were selected for analysis and scrubbed with a wire brush in distilled water to remove adhering sediment. Sample size was limited once the minimum number of individuals (MNI) was determined within the material available from each stratigraphic unit of interest (Early, Middle, and Late). The exterior surface of each shell was treated with 0.5 N HCl to remove contaminants and postdepositionally altered carbonate, rinsed in distilled water, and dried overnight. Samples were obtained from the outer layer of each shell using a dental drill (0.5-mm bit).

After inspecting the sample under the microscope to identify any foreign material, the powder was placed in a labeled glass vial. The drill bit was cleaned in a sonicated ethanol bath between samples to avoid cross-contamination. Thirty-nine edge samples for seasonality were drilled at intact sections of the growth margin. One of these shells was incrementally sampled (2.0-mm spacing) through its growth to establish the seasonal range of oxygen-isotope measures. This was done to confirm habitat similarity based on previous work in the Acapetahua region and to contextualize seasonality determination (Figure 5.6; see also Chapter 5).

The oxygen-isotope composition of shell carbonate samples was measured at the College of Oceanic and Atmospheric Sciences at Oregon State University using a Finnigan MAT 252 mass spectrometer and a Kiel-III online acid digestion system (Mix 2005). This system automatically reacts carbonate samples in individual sample vials with 100-percent H_3PO_4 *in vacuo* at 70° C, and cryogenically pumps the evolved CO_2 to the dual micro-inlet of the mass spectrometer. Average internal precision of carbonate analyses for oxygen-isotope and carbon-isotope measurements was (respectively) ± 0.02 per mil and ± 0.01 per mil.

External precision of replicate analyses of a local carbonate standard (known as Wiley marble) was run daily on this system in the same size range as the samples. Over the same time interval, this measurement was ± 0.06 per mil for the oxygen-isotope measurement and ± 0.02 per mil for the carbon-isotope measurement (± 1 standard deviation, $n = 722$). Calibration of measured isotopic values to the Vienna Pee Dee Belemnite (VPDB) standard was done via certified carbonate standards provided by the U.S. National Institute of Standards and Technology (NIST).

Primary calibration is based on the isotopic values and precision obtained for NIST-8544 (also known as NBS-19 limestone).

RESULTS AND INTERPRETATION

Oxygen-isotope data for *P. radiata* shells from El Varal are presented in Table 13.1 (profile data) and Table 13.2 (edge samples). The oxygen-isotope profile of one shell from the middle of the archaeological sequence ranges from -10.50 to -3.11 per mil, respectively, for wet and dry seasons. These data clearly show that this mollusk species lived in a brackish water environment that was heavily influenced by freshwater influx during wet-season months—an environmental setting analogous to that of the modern *P. radiata* populations analyzed by Kennett and Voorhies (1995, 1996) in the Acapetahua region. The existence of this species throughout the sequence suggests that a similar habitat existed in the vicinity of El Varal. The appearance of mollusk species from more distant marine habitats in the upper sections of the site suggests subsistence diversification in the context of resource depression, environmental change (e.g., loss of habitat due to lagoon in-filling), or both (see Chapter 5 for a more detailed analysis of habitats exploited).

Shell margin values from El Varal ($n = 39$) are plotted in Figure 13.3 against the entire range of oxygen-isotope variability exhibited by the archaeological specimens. These values extend across the full range of oxygen-isotope variability (-10.5 to -2 per mil) and indicate prehistoric collection throughout the year, with a clear emphasis during dry-season months (approximately -6 to -2 per mil).

Wet-season exploitation is only represented within the middle section of the sequence when these data are examined in greater stratigraphic detail. This could represent a temporary shift in seasonal harvesting strategies associated with more frequent visits to the site or perhaps with a resident population at this location collecting shellfish throughout the year. However, this interpretation should be viewed with caution due to the limited number of measurements available from each stratigraphic component. Dry-season exploitation of *P. radiata* is consistent with the idea that El Varal was used strategically during the year, when seasonal resource abundance was peaking in the estuarine zone.

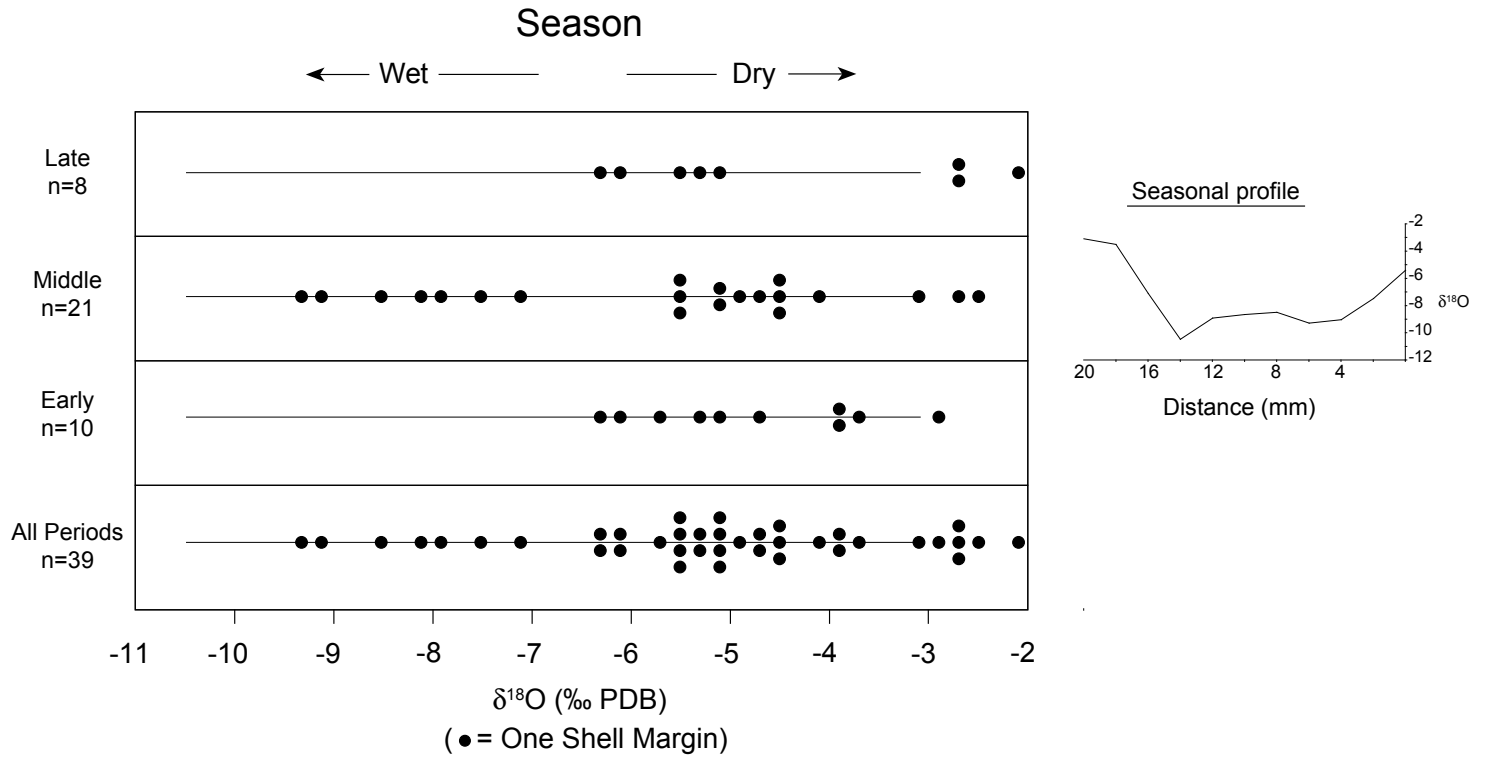


Figure 13.3. Summary of shell margin samples from each level analyzed at El Varal. The mid-sequence oxygen-isotope profile is included to show the full extent of seasonal variability.

Table 13.2. Stable-isotope values for shell margins of *Polymesoda radiata*

Sample No.	Unit/Level No.	Sequence No.	Stratigraphic Period	δ ¹³ C (PDB)	δ ¹⁸ O (PDB)
EVS13 Pr1 A	N75W0/1B	S13	Late	-6.33	-5.38
EVS13 Pr2 A	N75W0/1B	S13	Late	-2.12	-5.19
EVS13 Pr3 A	N75W0/1B	S13	Late	-8.33	-5.54
EVS14 Pr1 A	N75W0/1C	S14	Late	-6.32	-6.20
EVS14 Pr2 A	N75W0/1C	S14	Late	-7.08	-6.34
EVS14 Pr3 A	N75W0/1C	S14	Late	-3.04	-2.76
EVS2 Pr1 A	N85W0/1	S2	Late	-3.95	-2.18
EVS2 Pr2 A	N85W0/1	S2	Late	-3.20	-2.67
EV3S23 Pr1 A	N35W0/4	S23	Middle	-8.06	-4.01
EV3S24 Pr1 A	N35W0/5	S24	Middle	-8.48	-2.41
EVS29 Pr1 A	N65W0/4	S29	Middle	-9.01	-4.64
EVS29 Pr2 A	N65W0/4	S29	Middle	-6.41	-9.36
EVS29 Pr3 A	N65W0/4	S29	Middle	-9.72	-2.71
EVS29 Pr4 A	N65W0/4	S29	Middle	-8.07	-4.49
EVS29 Pr5 A	N65W0/4	S29	Middle	-4.86	-4.86
EVS29 Pr6 A	N65W0/4	S29	Middle	-8.39	-7.14
EVS29 Pr7 A	N65W0/4	S29	Middle	-9.08	-7.82
EVS29 Pr8 A	N65W0/4	S29	Middle	-7.61	-8.05
EVS29 Pr9 A	N65W0/4	S29	Middle	-7.43	-8.41
EVS29 Pr10 A	N65W0/4	S29	Middle	-7.46	-4.42
EV1A	N65W0/4	S29	Middle	-8.53	-3.13
EV2A	N65W0/4	S29	Middle	-7.20	-5.42

Table 13.2. (continued)

Sample No.	Unit/Level No.	Sequence No.	Stratigraphic Period	$\delta^{13}\text{C}$ (PDB)	$\delta^{18}\text{O}$ (PDB)
EV3A	N65W0/4	S29	Middle	-7.80	-5.53
EV4A	N65W0/4	S29	Middle	-6.14	-4.49
EV5A	N65W0/4	S29	Middle	-7.71	-5.03
EV6A	N65W0/4	S29	Middle	-7.39	-9.15
EV7A	N65W0/4	S29	Middle	-7.40	-7.58
EV8A	N65W0/4	S29	Middle	-8.37	-5.42
EV9A	N65W0/4	S29	Middle	-7.25	-5.18
EVS43 Pr1 A	N55W0/4	S43	Early	-8.31	-2.90
EVS43 Pr2 A	N55W0/4	S43	Early	-9.89	-5.79
EVS43 Pr3 A	N55W0/4	S43	Early	-7.44	-6.24
EVS43 Pr4 A	N55W0/4	S43	Early	-9.01	-6.16
EVS43 Pr5 A	N55W0/4	S43	Early	-8.84	-4.68
EVS43 Pr6 A	N55W0/4	S43	Early	-6.36	-3.70
EVS43 Pr7 A	N55W0/4	S43	Early	-8.98	-5.22
EVS43 Pr8 A	N55W0/4	S43	Early	-8.18	-3.98
EVS43 Pr9 A	N55W0/4	S43	Early	-8.67	-3.81
EVS43 Pr10 A	N55W0/4	S43	Early	-8.40	-5.05